ARTICLE

A novel pathogenic mitochondrial DNA variant m.4344T>C in tRNA^{Gln} causes developmental delay

Xiaojie Yin[1,6], Qiyu Dong[1,6], Shuanglong Fan[1], Lina Yang[1], Hao Li[1], Yijun Jin[1], Mahlatsi Refiloe Laurentinah[1], Xiandan Chen[2], Aliaksei Sysa[2], Hezhi Fang[1], Jianxin Lyu[1,3]✉, Yongguo Yu[4,5]✉ and Ya Wang[1]✉

Mitochondrial diseases are a group of genetic diseases caused by mutations in mitochondrial DNA and nuclear DNA. However, the genetic spectrum of this disease is not yet complete. In this study, we identified a novel variant m.4344T>C in mitochondrial tRNA^{Gln} from a patient with developmental delay. The mutant loads of m.4344T>C were 95% and 89% in the patient's blood and oral epithelial cells, respectively. Multialignment analysis showed high evolutionary conservation of this nucleotide. TrRosettaRNA predicted that m.4344T>C variant would introduce an additional hydrogen bond and alter the conformation of the T-loop. The transmitochondrial cybrid-based study demonstrated that m.4344T>C variant impaired the steady-state level of mitochondrial tRNA^{Gln} and decreased the contents of mitochondrial OXPHOS complexes I, III, and IV, resulting in defective mitochondrial respiration, elevated mitochondrial ROS production, reduced mitochondrial membrane potential and decreased mitochondrial ATP levels. Altogether, this is the first report in patient carrying the m.4344T>C variant. Our data uncover the pathogenesis of the m.4344T>C variant and expand the genetic mutation spectrum of mitochondrial diseases, thus contributing to the clinical diagnosis of mitochondrial tRNA^{Gln} gene variants-associated mitochondrial diseases.

Journal of Human Genetics; https://doi.org/10.1038/s10038-024-01254-5

INTRODUCTION

Mitochondrial diseases are a group of common inherited metabolic diseases with a prevalence of approximately 1:5000, mainly caused by mitochondrial oxidative phosphorylation (OXPHOS) system defects [1]. The clinical phenotype of mitochondrial diseases is highly variable and heterogeneous, mainly including muscle weakness, nervous system involvement, developmental delay, retinitis pigmentosa, cardiac involvement and elevated blood lactic acid and pyruvate [2–5]. The OXPHOS system consists of five complexes embedded in the inner mitochondrial membrane (complex I-V) and two small electron carriers (ubiquinone and cytochrome c) [6]. Most proteins in the OXPHOS system are encoded by nuclear DNA (nDNA). Human mitochondrial DNA (mtDNA) is a double-chained ring molecule with a total length of 16,569 base pairs and encodes 37 genes essential for OXPHOS biogenesis, including two rRNAs (12S and 16S) and 22 tRNAs, along with 13 proteins corresponding to the subunits of OXPHOS complexes (I, III, IV and V) [7, 8]. With the application of next generation sequencing (NGS), approximately four hundred genes have been reported to be associated with mitochondrial disease [9, 10]. However, many patients with mitochondrial diseases are genetically undiagnosed, suggesting that many genetic mutations that cause the disease are yet to be identified.

The *MT-TQ* gene encodes the mitochondrial glutamine transfer RNA (tRNA^{Gln}), which functions to recognize and bind to glutamine, and then transport it to the correct position for protein synthesis [11]. To data, a total of 32 variants in *MT-TQ* have been reported in the Mitomap and ClinVar databases, as well as in the literature. Among these, m.4332G>A, m.4335C>T, m.4336T>C and m.4349C>T have been definitively confirmed as pathogenic variants.

In this study, we identified a novel pathogenic variant m.4344T>C in mitochondrial tRNA^{Gln} gene from a patient with developmental delay. The pathogenesis of this variant was verified by determining the mitochondrial tRNA levels, oxygen respiration, OXPHOS complexes contents, mitochondrial membrane potential, mitochondrial ATP and ROS productions in cybrid cells with and without the m.4344T>C variant.

MATERIAL AND METHODS

Patient and informed consent

The patient was admitted to Xinhua Hospital, Shanghai Jiao Tong University School of Medicine in June 2023. The study was conducted with the consent of the patient's guardian. All studies were done in agreement with the protocol of the ethics committee of Xinhua Hospital, Shanghai Jiao Tong University School of Medicine.

[1]Key Laboratory of Laboratory Medicine, Ministry of Education, Zhejiang Provincial Key Laboratory of Medical Genetics, School of Laboratory Medicine and Life sciences, Wenzhou Medical University, Wenzhou 325035 Zhejiang, China. [2]International Sakharov Environmental Institute of Belarusian State University, Minsk 220070, Republic of Belarus. [3]Laboratory Medicine Center, Department of Clinical Laboratory, Zhejiang Provincial People's Hospital, Affiliated People's Hospital, Hangzhou Medical College, Hangzhou 310053 Zhejiang, China. [4]Department of Pediatric Endocrinology and Genetics, Xinhua Hospital, Shanghai Jiao Tong University School of Medicine, Shanghai Institute for Pediatric Research, Shanghai 200092, China. [5]Shanghai Key Laboratory of Pediatric Gastroenterology and Nutrition, Shanghai 200092, China. [6]These authors contributed equally: Xiaojie Yin, Qiyu Dong ✉email: jxlu313@163.com; yuyongguo@shsmu.edu.cn; yawang@wmu.edu.cn

Received: 9 January 2024 Revised: 26 March 2024 Accepted: 17 April 2024
Published online: 10 May 2024

Whole exome sequencing and mitochondrial genomic sequencing

Whole exome sequencing (WES) sequencing and mitochondrial genomic sequencing were performed using Illumina HiSeq 2000 sequencer (Illumina, USA) [12, 13]. DNA was obtained from peripheral blood of the patient and his parents, and qualitative analysis was performed by agarose gel electrophoresis. After constructing the DNA library, the sequence was captured, and high-throughput sequencing was performed using Illumina HiSeq 2000 sequencer. Quality control was then performed on the original sequencing results, including removing low-quality sequence fragments, filtering out low-quality bases and low-coverage sequencing fragments. The sequence data were aligned to the human reference genome (GRCh38/hg38). Germline short variants (SNPs, insertions or deletions) were analyzed by the genome analysis toolkit (GATK). The pathogenicity of the variant was assessed by the filters such as allele frequency, and its effect on protein function, consistent with the pathogenesis of the recessive model.

Variants analysis

To verify the variant site and detect the mtDNA mutation loads, 1 mL of venous blood was collected from the patient and his parents. Oral epithelial cells were collected using a disposable throat swab. DNA was extracted using a small amount of genomic DNA extraction kit (Beyotime, China). Amplification primers were as follows: forward: 5′- CATACCCCC-GATTCCGCTAC-3′; reverse: 5′-TGTGATGAGTGTGCCTGCAA-3′. The DNA was amplified using Taq Plus Polymerase (Vazyme, China) and then sent for Sanger sequencing.

Pathogenicity prediction

To analyze the pathogenicity of m.4344T>C, we used ClustalW program to predict the conservation of sequences among different species [14]. The *MT-TQ* sequences of 14 vertebrate species from GenBank were analyzed. Human nucleotide sequences were compared with those of other animals to calculate CI [15]. The CI represents conservation between species, which is the percentage of species with wild-type nucleotides at the corresponding location. CI ≥ 75% is considered functionally important [16]. We further used trRosettaRNA website (http://yanglab.qd.sdu.edu.cn/trRosettaRNA/) to predict the effect of mutation on the tertiary structure of tRNA [17].

Cells generation and culture

Platelets were isolated from the patient's venous blood and fused with mtDNA-less ρ0 human osteosarcoma 143B cells, as described previously [18, 19]. Single cybrid clones were selected by culturing the fusion mixtures in a medium without uridine and sodium pyruvate. Mutant cells were selected by Sanger sequencing. In addition to the difference in heterogeneity, the clones have the same nDNA and mtDNA background, which can be used to explain the changes in cell function due to the presence of m.4344T>C. The cybrid cells were maintained in high-glucose Dulbecco's modified Eagle's medium (Gibco, USA), supplement with 10% cosmic calf serum (Gibco, USA), 1% (v/v) penicillin-streptomycin (Beyotime, China) and 0.25 μg/mL amphotericin B (Beyotime, China). The cybrid cells were cultured in an atmosphere of 5% CO_2 at 37 °C.

Blue native PAGE (BN-PAGE)

BN-PAGE was conducted as described before [20]. The cells were lysed with 20% TritonX-100 (Sigma, USA) for 20 min, followed by centrifugation at 20,000 × *g* for 20 min. The supernatant was absorbed to determine the concentration, and 6× loading was added to prepare the required sample at 4 °C. Next, the samples were separated using a 3.5%-16% gradient polyacrylamide gel. Subsequently, the proteins were transferred to a 0.22 μm PVDF membrane (Bio-Rad, USA). The membrane was incubated with 5% non-fat milk at room temperature for 1–2 h, and then incubated with the primary antibody overnight at 4 °C. Finally, the membrane was incubated with the secondary antibody at room temperature for 2 h. Protein signals were detected using the Super Signal West Pico chemiluminescent substrate (Thermo, USA). The following are the antibodies used: anti-GRIM19 (1:1000, Abcam, USA), anti-SDHA (1:3000, Abcam), anti-UQCRC2 (1:2000, Abcam); anti-MTCO1 (1:2000, Abcam); anti-ATP5A (1:3000, Abcam).

Oxygen consumption rate

The oxygen consumption in intact cells was measured using the oxygraphy-2k detector (Oroboros, Austria) as described before [21]. In brief, about 4×10^6 cells were collected during machine calibration and added to the machine after suspension in 200 μL 1 × TD buffer (25 mM Tris-Base, 137 mM NaCl, 10 mM KCl, 0.7 mM Na_2HPO_4, pH 7.4). After the basic respiratory value was stabilized, oligomycin (0.1 mg/mL, Sigma-Aldrich) was added to determine ATP-linked respiration. Finally, Cell numbers were used for calibration. To examine the activity of respiratory chain complexes, using 2% (w/v) digitonin to permeabilize cells [22]. The concentration was optimized to ensure mitochondrial viability prior to the experiment. Permeabilize good cells were collected and added to the machine after being rehung using 200 μL working buffer (20 mM HEPES, 250 mM Sucrose, 10 mM $MgCl_2$, 1 mM ADP, 2 mM KH_2PO_4, pH 7.1). Add the appropriate substrate and inhibitor when breathing is stable. After the basic respiratory value was stabilized, Glutamate (1 M, Sigma-Aldrich) and malate (1 M, Sigma-Aldrich) was added to measure complex I respiration. Complex I was inhibited with rotenone (100 μM, Sigma-Aldrich) before glycerol-3-phosphate (10 mM, Sigma-Aldrich) was added to support complex III respiration. After add antimycin A (10 mM, Sigma-Aldrich) to inhibit complex III, use TMPD (4 mM, Sigma-Aldrich) and ascorbate (1 M, Sigma-Aldrich) to stimulate the complex IV. Complex IV was inhibited with NaN_3 (4 M, Sigma-Aldrich). Finally, the number of cells was also used for calibration. Finally, we exported the O2 Flux per V [pmol/(s*ml)] data from chambers A and B of the O2K instrument, with a value recorded every 0.04 min. After reaching equilibrium, we calculated the average of 25 values within each 1-min interval and plotted a line chart based on these average values.

Mitochondrial ATP contents

Mitochondrial ATP contents were detected using ATP Determination Kit (Thermo, USA) according to the manufacturer's instructions. Briefly, cells were seeded in 6-well plates to approximately 80% confluence. The cells were then incubated in the incubator for 2 h with a recording buffer (156 mM NaCl, 3 mM KCl, 2 mM $MgSO_4$, 1.25 mM KH_2PO_4, 2 mM $CaCl_2$, 20 mM HEPES, pH 7.35) containing 2-DG and sodium pyruvate. After incubation, the cells were collected and resuspended in ATP extraction solution (100 mM Tris-base, 4 mM EDTA-Na_2, pH 7.75) and subjected to a 100 °C water bath for 90 s. The supernatant was mixed with the working solution and added to a 96-well white plate to detect self-luminescence at 560 nm. The final results were calibrated with protein concentration.

Mitochondrial ROS levels

Mitochondrial ROS levels were measured using MitoSOX red reagent (Thermo, USA) according to the manufacturer's instructions. Briefly, when the cell density in the six-well plate reached 80%, the cells were collected and resuspended in a working solution containing 5 μM MitoSOX reagent. They were then incubated at 37 °C for 30 minutes in the dark and washed three times with PBS. Finally, the fluorescence with excitation at 510 nm and emission at 580 nm was analyzed using flow cytometry.

Mitochondrial membrane potential

Mitochondrial membrane potential (MMP) was measured using tetramethylrhodamine (Thermo, USA), following the manufacturer's instructions. The stock solution of TMRM was diluted 1000 times with PBS, and then the working solution of 30 nM was configured with DMEM. When the cell density reached approximately 80%, the cells were collected and resuspended in a working solution. They were then incubated at 37 °C for 30 min in the dark and washed three times with PBS. Finally, the fluorescence with excitation at 488 nm and emission at 570 nm was analyzed using flow cytometry.

Mitochondrial tRNA levels

Dot-Blot was used to analysis mitochondrial tRNA level by using DIG Northern Starter Kit (Roche12039672910, Switzerland) [23, 24]. Total mitochondrial RNAs were obtained from mitochondria isolated from cybrid cell lines, 2 μL of the same amount of total mitochondrial RNAs were add to nylon membranes and dried at room temperature. The RNA spots were crosslinked to the nylon membranes using a UV Stratalinker with an energy of 1200 J/min. Subsequently, the membranes were hybridized with a specifically DIG-labeled probe. Following hybridization, membrane washing, sealing, incubation, color development, and exposure were conducted according to the kit protocol. After exposure, the probe on the membrane was stripped, and the next probe hybridization was carried out. The hybridization and quantification of density in each band were performed as detailed previously. DIG-labeled oligodeoxynucleotides

specific for mitochondrial tRNA^{Gln}, tRNA^{Ile}, tRNA^{His}, and 5S rRNA were synthesized by Tsingke Biotechnology Company (Hangzhou, China) with the following sequences: 5′-AGGACTATGAGAATCGAACCCATCCCTGAG-3′ (tRNA^{Gln}), 5′-AGAAATAAGGGGGTTTAAGCTCCTATTATT-3′ (tRNA^{Ile}), 5′-AAA-TAAGGGGTCGTAAGCCTCTGTTGTCAG-3′ (tRNA^{His}) and 5′-CTAATTAATTA-TAAGGCCAGGACCAAACCT-3′ (5S rRNA).

Statistical analysis

All experiments had at least three independent replicates, and the data were shown as mean ± standard error of mean (SEM). *P* values were calculated using independent Student's *t* test. The $P < 0.05$ was considered to have a significant difference.

RESULTS

Clinical data

The patient (II-1) was an 18-months old boy who was born in a healthy non-consanguineous Chinese family (Fig. 1a). His parents had normal developmental history and no family history of neurological diseases. He was born at full term, weighing 2.9 kg at birth and 43 cm tall. However, the child's growth and development were delayed after birth, and his weight growth was not good. When he was three months old, he underwent a month of rehabilitation treatment, which had a slight recovery effect. A brain magnetic resonance imaging (MRI) showed no significant abnormalities. Physical examination showed a slight reduction in head circumference (41 cm, normal range 43.7–51.6 cm). The body was symmetrical, and there was slightly more back body hair. The heart, chest, and abdomen showed no obvious abnormalities. Further laboratory examination revealed elevated lactate (2.7 mM, normal range 0.50–2.20 mM). Blood ammonemia was normal. Urine screening revealed vitamin B1 deficiency, glycerol kinase deficiency or secondary mitochondrial energy metabolism disorder. Whole exome sequencing (WES) did not identify any pathogenic variations that could explain the clinical phenotype or mutations of unknown clinical significance. However, mtDNA sequencing identified a novel variant, m.4344T>C, in the tRNA^{Gln} gene. Genetic sequencing of his parents was negative, and this variant had not been reported previously. The presence of m.4344T>C in the patient's blood cells was confirmed by Sanger sequencing (Fig. 1b). We further determined the mutation loads using Sanger sequencing, and found that the mutation loads were 95% and 89% in the patient's blood and oral epithelial cells, respectively. However, the m.4344T>C variant was not detected in the blood cells of his parents, suggesting the variant appeared de novo (Fig. 1b).

Pathogenicity assessment

To investigate the pathogenicity of the m.4344T>C variant, we used the following criteria: (1) mutation incidence <1%; (2) CI ≥ 75%, as established by Ruiz-Pesini and Wallace, and (3) mutations may affect

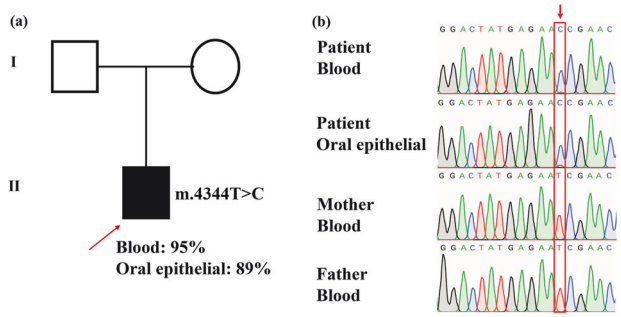

Fig. 1 Family pedigree and mutation loads analysis. **a** Segregation analysis of affected individual. Rectangles indicate males, circles female, and solid circle represents affected individual. The proband was pointed out by arrow; **b** The mutation loads of m.4344T>C in different tissues

the function of mt-tRNA genes. Therefore, we first performed a phylogenetic conservative analysis of this nucleotide. As shown in Fig. 2a, nucleotide at this site was highly conserved among different species, suggesting that the m.4344T>C variant was highly conserved with a conservation index (CI) of 100%. Additionally, it was worth noting that the m.4344T>C variant was located in the T-loop of the mitochondrial tRNA^{Gln} (Fig. 2b, c). It is predicted that this variant will introduce an additional hydrogen bond between bases at positions 58 and 55, altering the conformation of the T-loop, which might affect the stability of the tertiary structure and the efficiency of protein translation (Fig. 2d, e).

The m.4344T>C variant impaired the steady-state level of tRNA^{Gln} and mitochondrial complex I, III and IV contents

To fully explore the pathogenicity of the m.4344T>C variant, we constructed two cybrid cells by fusion of mtDNA-lacking ρo zero human osteosarcoma 143B cells with platelet from the patient: a wildtype cybrids (variant load was around 0%, marked as 4344T) and a homoplasmic mutant cybrids (variant load was around 100%, marked as 4344C) (Fig. 3a, b). To assess the impact of the m.4344T>C variant on the steady-state level of tRNA^{Gln}, total mitochondrial RNA was extracted from the cybrid cells and subjected to Dot-blot hybridization analysis with DIG-labeled oligodeoxynucleotides specific for tRNA^{Gln}, tRNA^{His}, tRNA^{Ile} and 5S rRNA (for nDNA transcription), respectively. As shown in Fig. 3c, d, the level of tRNA^{Gln} in the mutant cybrid cells obviously decreased to 56%, 56.5%, and 48% of that in the wild-type cybrid cells after normalization to tRNA^{His}, tRNA^{Ile}, and 5S rRNA, respectively. To further evaluate whether the m.4344T>C variant affected mitochondrial complexes contents, we conducted Blue Native PAGE (BN-PAGE)/immunoblot and found that the contents of complexes I, III and IV were significantly decreased in mutant cybrid cells compared to the wild-type cybrid cells (Fig. 3e, f). Altogether, these results suggested that the m.4344T>C variant impaired the steady-state level of tRNA^{Gln} and mitochondrial complex I, III and IV contents.

The m.4344T>C variant caused mitochondrial respiration deficiency

To further access whether the m.4344T>C variant affects cellular bioenergetics, we used oxygraphy-2k to measure the oxygen consumption rate, and found that a significant reduction in basal respiration and ATP-linked mitochondrial respiration in mutant cybrid cells compared to the wild-type cybrid cells (Fig. 4a, b), suggesting that m.4344T>C variant significantly decreased energy expenditure and mitochondrial oxidative capacity. Considering that the m.4344T>C variant impaired mitochondrial complex I, III and IV contents, we further measured complex I-, III-, and IV-mediated respiration in permeabilized cybrid cells by adding corresponding substrates and inhibitors. The results showed that the respiration mediated by complex I, III, and IV was remarkably decreased to 33.2%, 32.2%, and 47.5%, respectively, compared with the wild-type cybrid cells (Fig. 4c, d). These data indicated that the m.4344T>C variant caused mitochondrial respiration deficiency by damaging mitochondrial complexes I, III, and IV.

The m.4344T>C mutation resulted in decreased mitochondrial ATP level and mitochondrial membrane potential and aggravated mitochondrial ROS production

To further evaluate the effect of m.4344T>C mutation on mitochondrial function, we measured mitochondrial ATP levels and found that mitochondrial ATP levels were significant decreased in mutant cybrid cells compared to wild-type cybrid cells (Fig. 5a). In addition, we found a remarkable decrease in mitochondrial membrane potential and a significant increase in mitochondrial ROS production in mutant cybrid cells compared with wild-type cybrid cells. (Fig. 5b, c). Taken together, these data indicated that mitochondrial OXPHOS function was severely impaired in cybrid cells with the m.4344T>C mutation.

(a)

Organism	Acc-stem	D-stem	D-loop	D-stem	Ac-stem	Anticod -loop	Ac-stem	V-region	T-stem	T-loop	T-stem	Acc-stem	
Homo sapiens	TAGGATG	GG	GTGT	GAT	AGGTG	GCAC	G	GAGAA	TTTTGGA	TTCTC	AGGG	ATGGG	TTCGATT	CTCAT	AGTCCTA	G
Pongo abelii	TAGGATA	GG	GTGT	GAT	GGGTG	GCAC	G	GAGAA	TTTTGGA	TTCTC	AGGG	GTGGG	TTCAACT	CCCAT	AATCCTA	G
Pongo pygmaeus	TAGGATG	GG	GTGT	GAT	GGGTG	GCAC	G	GAGAA	TTTTGGA	TTCTC	AGGG	GTGGG	TTCAATT	CCCAT	AGTCCTA	G
Gorilla gorilla	TAGGATG	GG	GTGT	GAC	AGGTG	GCAC	G	GAGAA	TTTTGGA	TTCTC	AGGG	ATGGG	TTCAATT	CTCAT	AGTCCTA	G
Pan paniscus	TAGGATG	GG	GTGT	GAT	AGGTG	GCAC	G	GAGAA	TTTTGGA	TTCTC	AGGG	ATGGG	TTCGACT	CTCAT	AGTCCTA	G
Papio hamadryas	TAGGATG	GA	GTGT	GAG	GGGTA	GCAC	G	GAGAA	GTTTGGA	TTCTC	AGGA	GCAGG	TTCGATG	CCTGT	AATCCTA	G
Macaca mulatta	TAGGATA	GA	GTGT	GTA	GGGTA	GCAC	G	GAGAA	GTTTGGA	TTCTC	AGGG	GTAGG	TTCGATA	CCTAC	AGTCCTA	G
Macaca sylvanus	TAGGATG	GG	GTGT	ATG	AGGTA	GCAC	G	GAGAA	GTTTGGG	TTCTC	AGGG	GTAGG	TTCGATA	CCTAC	AGTCCTA	G
Pan troglodytes	TAGGATG	GG	GTGT	GAT	AGGTG	GCAC	G	GAGAA	TTTTGGA	TTCTC	AGGG	ATGAG	TTCGATT	CTTAT	AGTCCTA	G
Nycticebus coucang	TAGGACT	TG	GTGT	ATT	TGGTA	GCAC	G	AAGAA	TTTTGAA	TTCTT	AAGA	GTAGG	TTCAAGC	CCTAA	GGTTCTA	G
Tarsius bancanus	TAGAATA	TT	GTGT	AATT	GGGTA	GCAC	G	AAGAA	TTTTGGA	TTCTT	AAGT	ATAGG	TTCAATT	CCTGT	AATTCTA	G
Hylobates lar	TAGAACA	GG	GTGC	GAC	GGGTG	GCAC	G	GAGAG	TTTTGGG	TTCTC	AGGG	ATGGG	TTCGACT	CCTAT	GGTTCTA	G
Cebus albifrons	TAGGGTA	TG	GTGT	AAT	AGGTA	GCAC	G	GAGGA	TTTTGAG	TTCTT	AGGA	ATAGG	TTCGAGT	CCTAT	AATTCTA	G
Lemur catta	TAGAATA	GG	GTGT	GTTTTAGGTA		GCAC	G	AAGGA	CTTTGAA	TCCTT	AAGA	GACGG	TTCGATC	CCTGT	GATTCTA	G

(b)

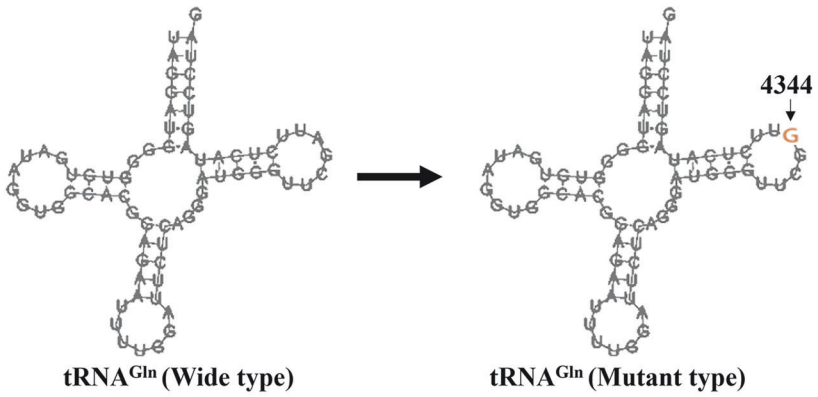

(c)

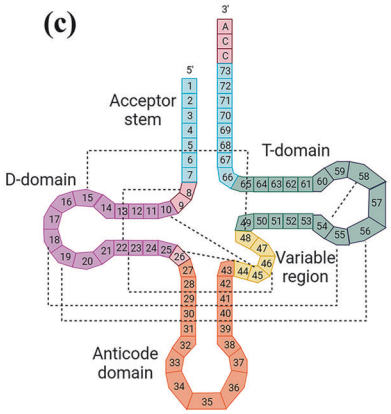

(d)

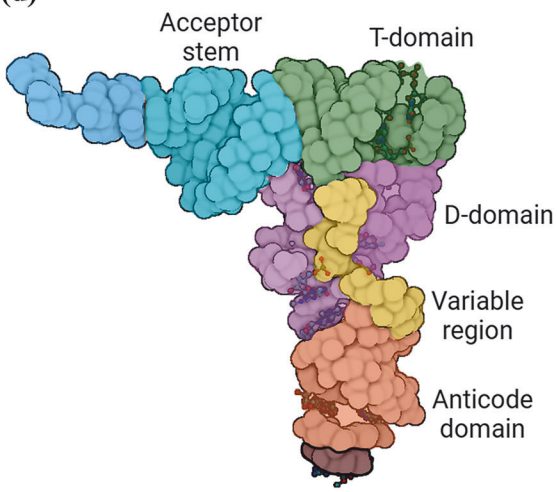

(e)

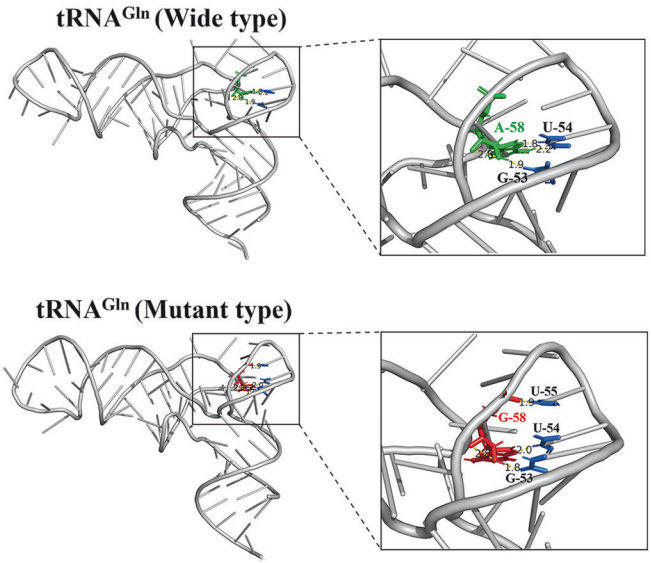

Fig. 2 Molecular analysis of the m.4344T>C variant in tRNA^{Gln} gene. **a** Suquence alignment of *MT-TQ* gene among different species. The arrow indicated the conservation of the A nucleotide at position 4344 throughout the species; **b** Cloverleaf structures of tRNA^{Gln}. Arrows indicate the position of the m.4344T>C variant; **c** Classic tRNA secondary structure; **d** Schematic model for the tertiary structure of tRNA^{Gln}. The acceptor stem, T-domain, D-domain, variable region and anticode domain of tRNA^{Gln} are shown in blue, green, purple, yellow and orange, respectively; **e** The intrinsic conformation of the T-loop might be affected by the hydrogen bond formation caused by m.4344T>C variant

Literature review and the combination clinical phenotype of *MT-TQ* mutations

To investigate the clinical phenotypic spectrum caused by *MT-TQ* mutations, we reviewed all the relevant literatures. Among the reported thirty-two mutations, only three mutations had detailed clinical information [25–27] (Table 1). These three mutations were m.4332G>A in the acceptor stem, m.4349C>T in the T-stem and m.4369A>AA in the anticodon domain of mitochondrial tRNA^{Gln}. The age of onset for patients with these mutations ranged from 5 to 20 years. The patient with the m.4332G>A mutation initially presented with sensorineural deafness. The patient with the m.4349C>T mutation experienced developmental delays at 15

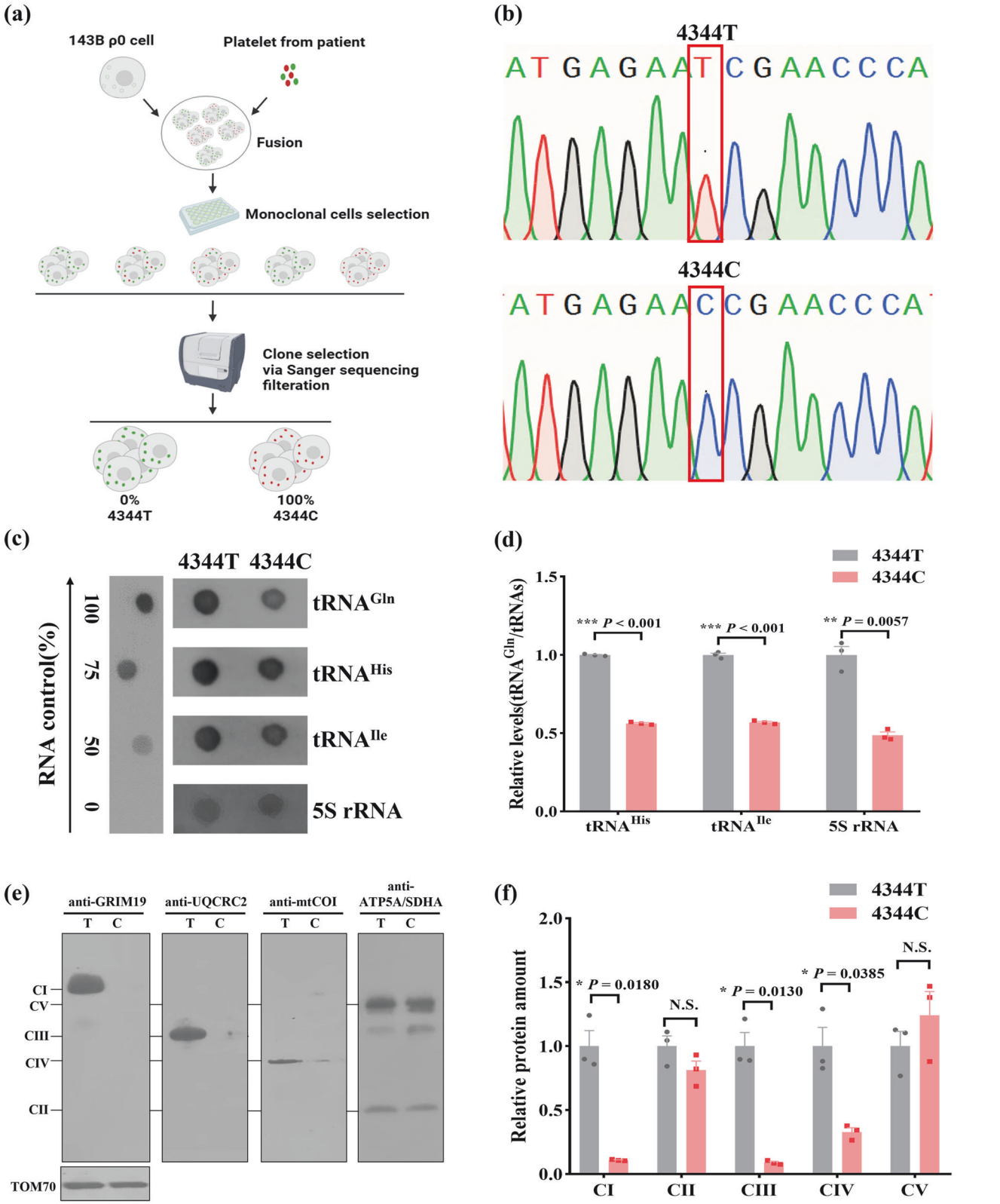

Fig. 3 The m.4344T>C variant impaired the steady-state level of $tRNA^{Gln}$ and mitochondrial OXPHOS complex I, III and IV contents. **a** Schematic diagram of monoclonal selection. Different colors indicate different mutations in the mtDNA. Green: m.4344T; red: m.4344C; **b** Sanger sequencing of cell models; **c**, **d** Dot-blot analysis of tRNA and quantification of tRNA levels in cybrid cells. The four dots on the far left represent the hybridization results of RNA with DIG-labeled actin probes at different concentrations. The relative average content of $tRNA^{Gln}$ in mutant cybrid cells are normalized to the content of $tRNA^{His}$, $tRNA^{Ile}$ and 5S rRNA in wild-type cybrid cells, respectively; **e**, **f** Blue Native PAGE analysis of mitochondrial complex I, II, III, IV, and V with anti-Grim19, anti-SDHA, anti-UQCRC2, anti-MTCOI and anti-ATP5A antibodies, respectively. The level of Tom70 was used as the internal control. Quantitative data were generated from three independent experiments and presented as the mean ± SEM. N.S. $P > 0.05$, $^{*}P < 0.05$, $^{**}P < 0.01$, $^{***}P < 0.001$

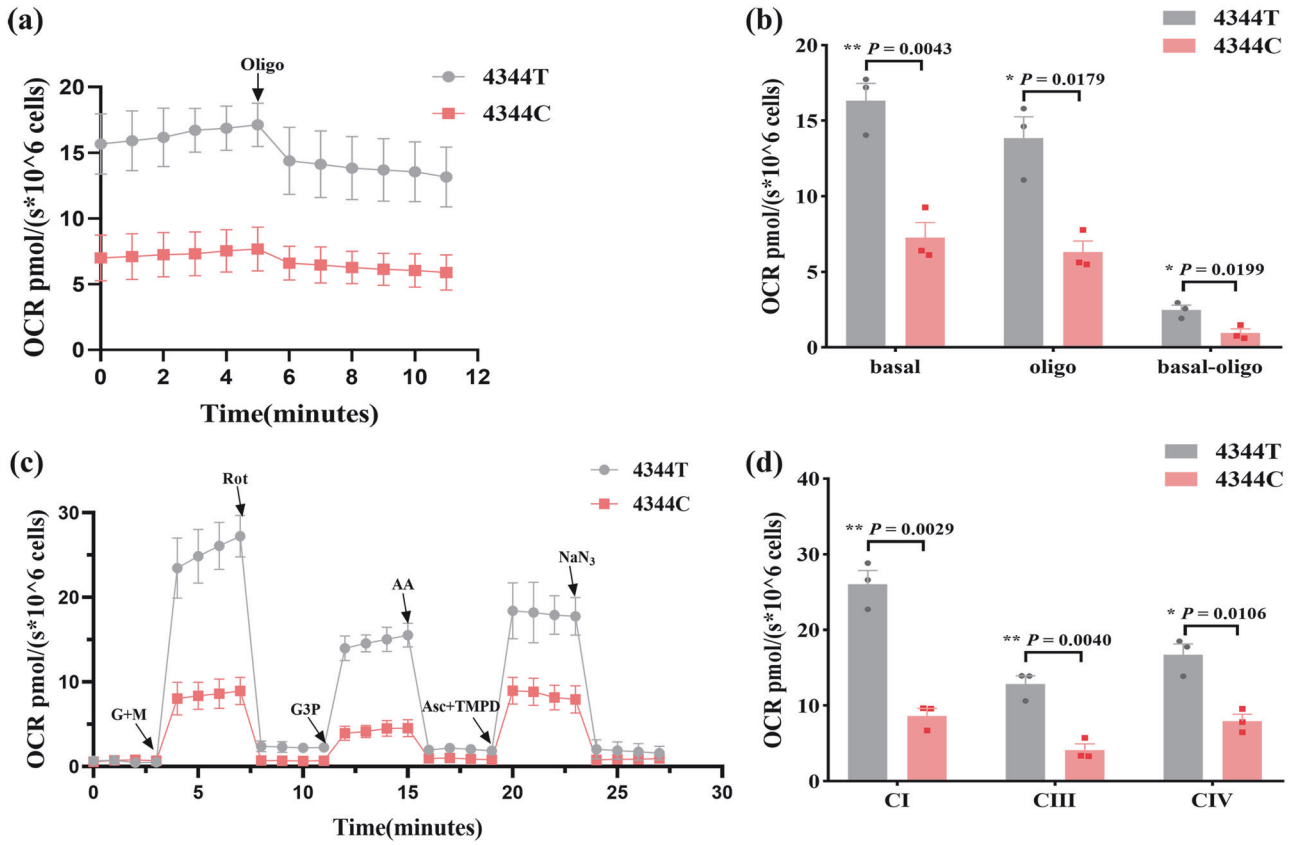

Fig. 4 The m.4344T>C variant triggered mitochondrial respiration deficiency. **a**, **b** Oxygen respiration rate (OCR) of the mutant and wild-type cybrid cells; **c**, **d** Oxygen respiration rate (OCR) mediated by complex I, III and IV in the mutant and wild-type cybrid cells. Cells were permeabilized with digitonin and then add corresponding substrates and inhibitors. Quantitative data were generated from three independent experiments and presented as the mean ± SEM. *$P < 0.05$, **$P < 0.01$

months old, followed by sensorineural deafness and recurrent headaches. Another possible pathogenic mutation, m.4369A>AA, was associated with muscle weakness and bilateral ptosis in the patient's phenotype. It seemed that common symptoms in patients with *MT-TQ* mutations included sensorineural deafness (67%, 2/3), muscle symptoms (67%, 2/3) and hearing problems (67%, 2/3). The newly identified individual (II-1) in our study presented with developmental delay, which might be an early symptom of mitochondrial disease.

DISCUSSION

In this study, we identified a novel pathogenic mutation m.4344T>C in $tRNA^{Gln}$ from an 18-months-old boy with developmental delay. The m.4344T>C mutation was found to be heteroplasmic in the available tissues, with a high mutant load of 95% and 89% in the patient's blood and oral epithelial cells, respectively. Multialignment analysis showed that this nucleotide was highly evolutionarily conserved among different species. TrRosettaRNA predicted that the m.4344T>C variant would alter the hydrogen bond, potentially affecting the stability of tertiary structure and the efficiency of protein translation. Functional studies demonstrated that the m.4344T>C mutation impaired the steady-state level of $tRNA^{Gln}$ and caused decreased mitochondrial respiratory chain complexes I, III and IV contents, which in turn resulted in mitochondrial dysfunction. Our study indicated that m.4344T>C was a pathogenic variant.

To date, 32 variants (m.4332G>A [25], m.4335C>T [28], m.4336T>C [28], m.4339G>A [29], m.4340A>G [29], m.4343A>G [30], m.4345C>T [31], m.4349C>T [26], m.4350C>T [29], m.4353T>C [32], m.4360G>A [29], m.4363T>C [33], m.4369A>G [33], m.4369A>AA [27], m.4370T>C [34], m.4371T>C [29], m.4372C>T [29], m.4373T>C [33], m.4375C>T [35], m.4381A>G [29], m.4384T>C [29], m.4385A>G [33], m.4385A>T [29], m.4386T>C [33], m.4387C>A [29], m.4388A>G [29], m.4392C>T [31], m.4393C>T [30], m.4394C>T [33], m.4395A>G [36], m.4399T>C [29] and m.4400A>G [29]) in $tRNA^{Gln}$ gene have been reported, of which the m.4332G>A, m.4335C>T, m.4336T>C and m.4349C>T variants were the confirmed pathogenic variants. The patient harboring the m.4332G>A variant presented with sensorineural deafness since the age of 20 years and experienced acute aphasia and right hemiparesis at the age of 47 years [25]. The patient carrying m.4335C>T or m.4336T>C variant was diagnosed with Parkinson's disease, and the activity of MMP and ATP synthesis in patient-derived lymphocytes decreased. The patient with the m.4349C>T variant experienced mild developmental delays at 15 months old and was able to walk independently, although not as stably as his peers. He also complained of unexplained vomiting since the age of 3 and began to suffer from sensorineural deafness and recurrent headaches at the age of 6 years. At the age of 12 years, he measured 128 cm in height and weighed 17 kg with hairy lower limbs. MRI of his brain showed significant cerebral atrophy [26]. The m.4369A>AA variant in mitochondrial $tRNA^{Gln}$ gene were another possible pathogenic variant according to the MitoTIP tRNA scoring. The patient with the m.4369A>AA variant experienced muscle weakness and bilateral ptosis at the age of 12 years [27]. In this study, our patient harboring the m.4344T>C variant was 18 months old and presented with developmental delay. It seemed that developmental delay was an early symptom, gradually progressing into

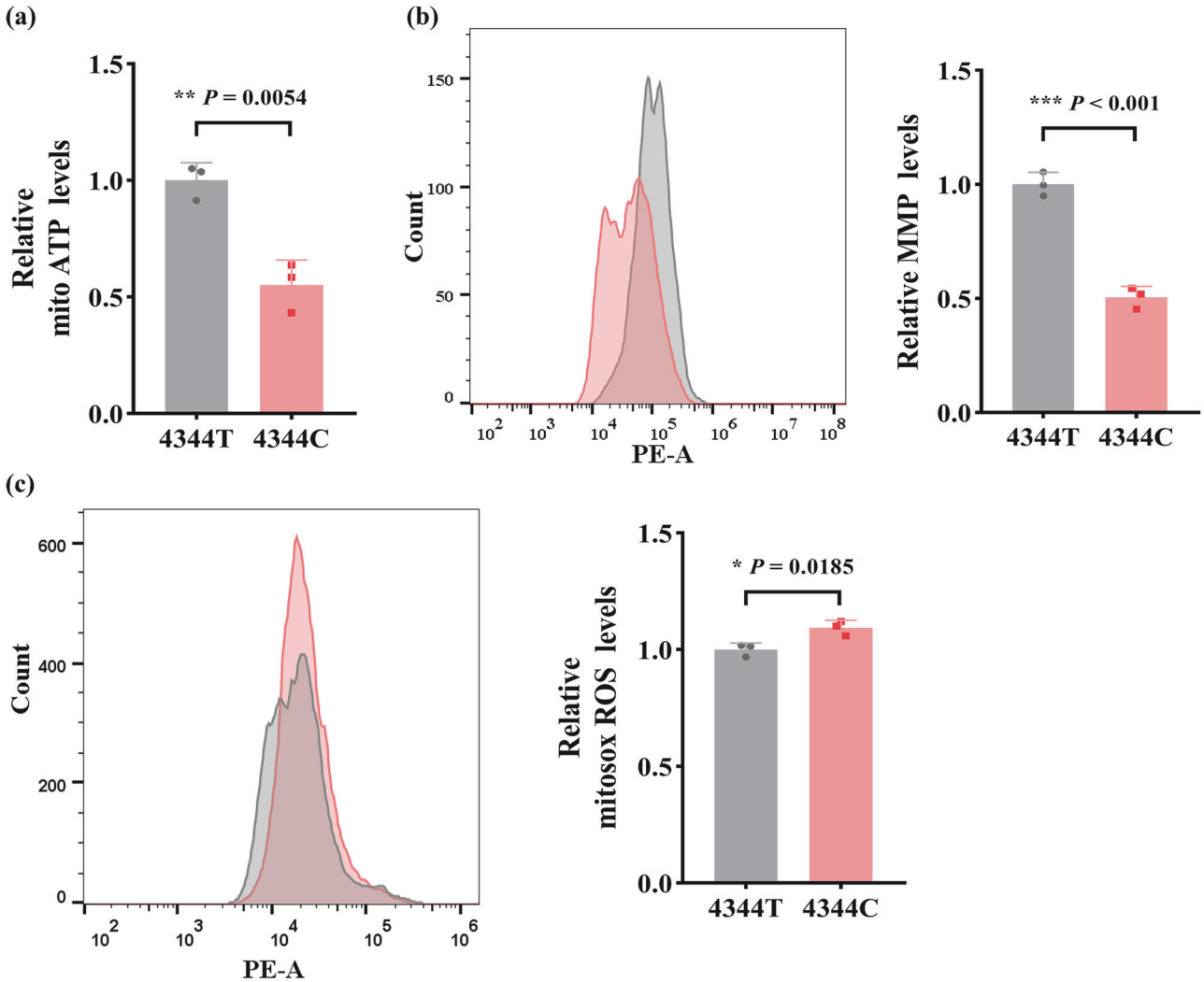

Fig. 5 The effect of m.4344T>C variant on mitochondrial ATP, MMP and ROS levels. **a** Mitochondrial ATP levels, **b** MMP levels and **c** mitochondrial ROS production in the mutant and wild-type cybrid cells. Quantitative data were generated from three independent experiments and presented as the mean ± SEM. *$P < 0.05$, **$P < 0.01$, ***$P < 0.001$

deafness, encephalopathy and muscle weakness in patients with mitochondrial tRNA^{Gln} gene variants.

Mt-tRNAs have played a crucial role in transporting amino acids and participating in protein synthesis within mitochondria [37]. Variants in mt-tRNAs may disrupt its processing and impair mitochondrial respiratory chain complexes (I, III, IV and V) contents, thus resulting in mitochondrial dysfunction [38]. The m.4349C>T variant in tRNA^{Gln} gene caused the mitochondrial respiratory chain complexes I and IV deficiency by decreasing the protein levels of CO1, ND1, CYB, and NDUFB8, and thus lead to mitochondrial dysfunction [33]. In this study, the m.4344T>C variant was heteroplasmic with a high mutant load of 95% and 89% in the patient's blood and oral epithelial cells, respectively. Multialignment analysis showed that this nucleotide was highly evolutionarily conserved. The m.4344T>C variant caused a change in the ribonucleic acid sequence from A to G at the T loop region of tRNA^{Gln} gene, which was crucial for maintaining the L-shaped structure and modification of the tRNA molecule [39–41]. TrRosettaRNA predicted that the m.4344T>C variant would alter hydrogen bond, potentially affecting the stability of the tertiary structure and the efficiency of protein translation. Functional studies showed that the m.4344T>C variant impaired the steady-state level of tRNA^{Gln} and decreased the contents of mitochondrial complexes I, III and IV, thereby leading to a significant reduction in basal respiration and ATP-linked mitochondrial respiration. Impaired mitochondrial respiratory function caused decreased cellular ATP levels and increased electron leakage, resulting in elevated oxidative stress levels and subsequent collapse of mitochondrial membrane potential. Consistently, the mutant cybrid cells carrying the m.4344T>C variant exhibited elevated mitochondrial ROS levels, reduced mitochondrial membrane potential and decreased cellular ATP levels compared to wild-type cybrid cells. These data indicated that the m.4344T>C variant impaired translation machinery of mitochondrial tRNA^{Gln}, thereby resulting in severe mitochondrial dysfunction.

In conclusion, we identify a novel pathogenic variant m.4344T>C in mitochondrial tRNA^{Gln} gene from an 18-months-old boy with developmental delay. The m.4344T>C variant results in a decreased steady-state level of tRNA^{Gln} and impaired mitochondrial OXPHOS complexes I, III and IV, leading to mitochondrial dysfunction. Our study expands the genetic variant spectrum of mitochondrial diseases, and provides a better understanding of the phenotypes associated with mitochondrial tRNA^{Gln} gene variants, thereby contributing to the clinical diagnose of mitochondrial tRNA^{Gln} gene variants-associated mitochondrial diseases.

Table 1. Detailed clinical manifestations of patients with *MT-TQ* variants

Patient		P1	P2	P3	P4
Genetic defects		m.4369A>AA	m.4332G>A	m.4349C>T	m.4344T>C
Age of onset (y)		5	20	6	1.5
Initial clinical manifestation		muscle weakness and bilateral ptosis	sensorineural deafness	sensorineural deafness and recurrent headache	developmental delay
Heteroplasmy level		87% in limb muscles 61% in ocular muscles 23% in fibroblasts	81% in muscle	94.3% in muscle 55% in peripheral blood 75% in urinary sediment	89% in oral epithelial 95% in peripheral blood
Neurological manifestations	Recurrent headaches	NA	NA	+	NA
	Learning disability	NA	NA	NA	NA
	Dementia	NA	NA	NA	NA
	Seizures	NA	+	NA	NA
	Stroke-like episodes	NA	+	+	NA
Ear	Hearing impairment	NA	+	+	NA
Eye	Visual disturbance	−	NA	NA	NA
Muscle	Fatigue	+	+	−	NA
	Exercise intolerance	+	+	−	NA
	Myopathy	+	+	−	NA
Imageological examination	MRI/CT	NA	+	+	−
Laboratorial examination	Lactic acidosis	NA	+	−	+
OXPHOS complexes activities or contents		CIV↓ *	CIV↓ *	CI and CIV↓ * CI↓ **	CI, CIII and CIV↓ **
Ref.		[27]	[25]	[26]	The current patient

− negative, + positive, *NA* not available or not described, *y* year-old or years, *Ref.* Referance, * muscles, ** cybrids, ↓ decreased

REFERENCES

1. Zhang T-g, Miao C-y. Mitochondrial transplantation as a promising therapy for mitochondrial diseases. Acta Pharmaceutica Sin B. 2023;13:1028–35.
2. Gorman GS, Chinnery PF, DiMauro S, Hirano M, Koga Y, McFarland R, et al. Mitochondrial diseases. Nat Rev Dis Prim. 2016;2:1–22.
3. Craven L, Alston CL, Taylor RW, Turnbull DM. Recent advances in mitochondrial disease. Annu Rev Genomics Hum Genet. 2017;18:257–75.
4. Alston CL, Rocha MC, Lax NZ, Turnbull DM, Taylor RW. The genetics and pathology of mitochondrial disease. J Pathol. 2017;241:236–50.
5. Schapira AH. Mitochondrial disease. Lancet. 2006;368:70–82.
6. Fernandez-Vizarra E, Zeviani M. Mitochondrial disorders of the OXPHOS system. FEBS Lett. 2021;595:1062–106.
7. Suzuki T, Nagao A, Suzuki T. Human mitochondrial tRNAs: biogenesis, function, structural aspects, and diseases. Annu Rev Genet. 2011;45:299–329.
8. DiMauro S, Davidzon G. Mitochondrial DNA and disease. Ann Med. 2005;37:222–32.
9. Stenton SL, Prokisch H. Genetics of mitochondrial diseases: Identifying mutations to help diagnosis. EBioMedicine. 2020;56:102784.
10. Mavraki E, Labrum R, Sergeant K, Alston CL, Woodward C, Smith C, et al. Genetic testing for mitochondrial disease: the United Kingdom best practice guidelines. Eur J Hum Genet. 2023;31:148–63.
11. Karakaidos P, Rampias T. Mitonuclear interactions in the maintenance of mitochondrial integrity. Life. 2020;10:173.
12. Fang H, Hu N, Zhao Q, Wang B, Zhou H, Fu Q, et al. mtDNA haplogroup N9a increases the risk of type 2 diabetes by altering mitochondrial function and intracellular mitochondrial signals. Diabetes. 2018;67:1441–53.
13. Du M, Wei X, Xu P, Xie A, Zhou X, Yang Y, et al. A novel mitochondrial m. 14430A> G (MT-ND6, p. W82R) variant causes complex I deficiency and mitochondrial Leigh syndrome. Clin Chem Lab Med. 2020;58:11809–17.
14. Thompson JD, Gibson TJ, Higgins DG. Multiple sequence alignment using ClustalW and ClustalX. Curr Protocols Bioinformatics. 2003;2.3.1-2.3.22.
15. Bartoszewicz JM, Seidel A, Renard BY. Interpretable detection of novel human viruses from genome sequencing data. NAR Genomics Bioinforma. 2021;3:lqab004.
16. Xue L, Wang M, Li H, Wang H, Jiang F, Hou L, et al. Mitochondrial tRNA mutations in 2070 Chinese Han subjects with hypertension. Mitochondrion. 2016;30:208–21.
17. Wang W, Feng C, Han R, Wang Z, Ye L, Du Z, et al. trRosettaRNA: automated prediction of RNA 3D structure with transformer network. Nat Commun. 2023;14:7266.
18. Zhou X, Lou X, Zhou Y, Xie Y, Han X, Dong Q, et al. Novel biallelic mutations in TMEM126B cause splicing defects and lead to Leigh-like syndrome with severe complex I deficiency. J Hum Genet. 2023;68:239–46.
19. Fang H, Ye X, Xie J, Li Y, Li H, Bao X, et al. A membrane arm of mitochondrial complex I sufficient to promote respirasome formation. Cell Reports. 2021;35:108963.
20. Lou X, Zhou Y, Liu Z, Xie Y, Zhang L, Zhao S, et al. De novo frameshift variant in MT-ND1 causes a mitochondrial complex I deficiency associated with MELAS syndrome. Gene. 2023;860:147229.
21. Fang H, Xie A, Du M, Li X, Yang K, Fu Y, et al. SERAC1 is a component of the mitochondrial serine transporter complex required for the maintenance of mitochondrial DNA. Sci Transl Med. 2022;14:eabl6992.
22. Hayes P, Fergus C, Ghanim M, Cirzi C, Burtnyak L, McGrenaghan C. Queuine Micronutrient Deficiency Promotes Warburg Metabolism and Reversal of the Mitochondrial ATP Synthase in Hela Cells. Nutrients. 2020;12:2020.
23. Cheley S, Anderson R. A reproducible microanalytical method for the detection of specific RNA sequences by dot-blot hybridization. Anal Biochem. 1984;137:15–9.
24. Meng F, Jia Z, Zheng J, Ji Y, Wang J, Xiao Y, et al. A deafness-associated mitochondrial DNA mutation caused pleiotropic effects on DNA replication and tRNA metabolism. Nucleic Acids Res. 2022;50:9453–69.
25. Bataillard M, Chatzoglou E, Rumbach L, Sternberg D, Tournade A, Laforet P, et al. Atypical MELAS syndrome associated with a new mitochondrial tRNA glutamine point mutation. Neurology. 2001;56:405–7.
26. Ji K, Wang W, Lin Y, Xu X, Liu F, Wang D, et al. Mitochondrial encephalopathy Due to a Novel Pathogenic Mitochondrial tRNAGln m. 4349C> T Variant. Ann Clin Transl Neurol. 2020;7:980–91.
27. Dey R, Tengan CH, Morita MP, Kiyomoto BH, Moraes CT. A novel myopathy-associated mitochondrial DNA mutation altering the conserved size of the tRNA(Gln) anticodon loop. Neuromuscul Disord. 2000;10:488–92.
28. Venkatesan D, Iyer M, Raj N, Gopalakrishnan AV, Narayanasamy A, Kumar NS, et al. Assessment of tRNAThr and tRNAGln Variants and Mitochondrial Functionality in Parkinson's Disease (PD) Patients of Tamil Nadu Population. J Mol Neurosci. 2023;73:912–20.
29. Wong L-JC, Chen T, Wang J, Tang S, Schmitt ES, Landsverk M, et al. Interpretation of mitochondrial tRNA variants. Genet Med. 2020;22:917–26.
30. Zheng J, Bai X, Xiao Y, Ji Y, Meng F, Aishanjiang M, et al. Mitochondrial tRNA mutations in 887 Chinese subjects with hearing loss. Mitochondrion. 2020;52:163–72.
31. Zhu H-Y, Wang S-W, Liu L, Chen R, Wang L, Gong X-L, et al. Genetic variants in mitochondrial tRNA genes are associated with essential hypertension in a Chinese Han population. Clin Chim acta. 2009;410:64–9.
32. Qiu Q, Li R, Jiang P, Xue L, Lu Y, Song Y, et al. Mitochondrial tRNA mutations are associated with maternally inherited hypertension in two Han Chinese pedigrees. Hum Mutat. 2012;33:1285–93.
33. Jiang P, Ling Y, Zhu T, Luo X, Tao Y, Meng F, et al. Mitochondrial tRNA mutations in Chinese children with tic disorders. Biosci Rep. 2020;40:BSR20201856.
34. Ruiz-Pesini E, Wallace DC. Evidence for adaptive selection acting on the tRNA and rRNA genes of human mitochondrial DNA. Hum Mutat. 2006;27:1072–81.
35. Chen H, Sun M, Fan Z, Tong M, Chen G, Li D, et al. Mitochondrial C4375T mutation might be a molecular risk factor in a maternal Chinese hypertensive family under haplotype C. Clin Exp Hypertens. 2018;40:518–23.
36. Zarrouk-Mahjoub S, Mehri S, Ouarda F, Finsterer J, Boussaada R. Mitochondrial tRNA glutamine variant in hypertrophic cardiomyopathy. Herz. 2015;40:436–41.
37. Sissler M, González-Serrano LE, Westhof E. Recent advances in mitochondrial aminoacyl-tRNA synthetases and disease. Trends Mol Med. 2017;23:693–708.
38. Richter U, McFarland R, Taylor RW, Pickett SJ. The molecular pathology of pathogenic mitochondrial tRNA variants. FEBS Lett. 2021;595:1003–24.
39. Heidari MM, Khatami M, Kamalipour A, Kalantari M, Movahed M, Emmamy MH, et al. Mitochondrial mutations in protein coding genes of respiratory chain including complexes IV, V, and mt-tRNA genes are associated risk factors for congenital heart disease. EXCLI J. 2022;21:1306.
40. Tamaki S, Tomita M, Suzuki H, Kanai A. Systematic analysis of the binding surfaces between tRNAs and their respective aminoacyl tRNA synthetase based on structural and evolutionary data. Front Genet. 2018;8:227.
41. Powell CA, Nicholls TJ, Minczuk M. Nuclear-encoded factors involved in post-transcriptional processing and modification of mitochondrial tRNAs in human disease. Front Genet. 2015;6:79.

ACKNOWLEDGEMENTS

We sincerely thank the patient and his family who participated in the study. This work was supported by grants from the National Natural Science Foundation of China-excellent young scientists fund (No. 82222043), the Natural Science Foundation of China (No. U22A20342 and 82302636), the "Pioneer" and "Leading Goose" R&D Program of Zhejiang Province (No. 2024C03152), Zhejiang Provincial Natural Science Foundation (No. LQ23H200001), Scientific Research Fund of Zhejiang Provincial Education Department (No. Y202249698), Shanghai Municipal Commission of Health and Family Planning (No. 20204Y0451), Shanghai Scientific and Technological Innovation Action Plan (No.21YF1437800), Shanghai Natural Science Foundation of China (No.21ZR1452700) and the Science and Technology Bureau of Wenzhou (No.Y2023089).

COMPETING INTERESTS

The authors declare no competing interests.

ADDITIONAL INFORMATION

Correspondence and requests for materials should be addressed to Jianxin Lyu, Yongguo Yu or Ya Wang.